PAPER • **OPEN ACCESS**

Speculation of local aerodynamic loads on helicopter rotor blade in forward flight

To cite this article: Abdallah Dayhoum *et al* 2019 *IOP Conf. Ser.: Mater. Sci. Eng.* **610** 012099

View the article online for updates and enhancements.

This content was downloaded from IP address 195.43.0.86 on 12/09/2021 at 10:22

IOP Conf. Series: Materials Science and Engineering **610** (2019) 012099 doi:10.1088/1757-899X/610/1/012099

Speculation of local aerodynamic loads on helicopter rotor blade in forward flight

Abdallah Dayhoum[1], Mohamed Y. Zakaria[2], A. M. Elshabka[3] and O. E. Abdelhamid[4]

[1]MSc. Student, Military Technical College, Aerospace Engineering Department, 11766 Cairo, EGYPT
[2]Assistant Professor, Acting as department head, Military Technical College, Aerospace Engineering Department, 11766 Cairo, EGYPT
[3]Assistant Professor, Military Technical College, Aerospace Engineering Department, 11766 Cairo, EGYPT
[4]Professor, Military Technical College, Aerospace Engineering Department, 11766 Cairo, EGYPT

E-mail: A_Dayhoum@mtc.edu.eg

Abstract. Design of rotor blade is mainly the most important consideration in helicopter industry. A sufficient input data is needed for various flight conditions that should be accounted for in rotor design process. In this paper, blade element theory is applied to helicopter rotor blade in forward flight. The main objective is to assure the fidelity of using blade element theory in helicopter rotor blade design. Blade element theory is used for calculating the average lift, thrust, power for rotary wings and the local aerodynamic loads. The local non-dimensional normal force coefficients obtained from blade element theory were compared with experimental results of the 7A rotor at five non dimensional radial positions for the high speed test point 312. The results showed the same pattern of variation along the azimuth with a considered convergence along the blade radius.

1. Introduction

The helicopter is a flying vehicle that uses rotating wings for producing lift, propulsion, and the needed control to perform various missions. The relative motion between the blade surface and the air generates the aerodynamic forces. These forces, in contrast to fixed-wing airplanes, can be generated when the flight velocity is zero (hovering flight). Therefore vertical take-off and landing, or generally vertical flight, is a radical characteristic of the helicopter. Translational flight (forward, sideward or rearward flight) is conventionally a necessity so a propulsive force is prerequisite to oppose the fuselage and rotor drag which is a component of the total disc force and the other component, the thrust, is to overcome helicopter's weight.

Conventional rotors consist of two or more identical blades that are attached to a central hub. Lift and drag forces on these rotating blades generate the torque, thrust and other forces and moments on rotor. Rotary wing aircrafts development faced many problems along the time. In the very beginning, a reliable light engine was needed and the only available solution was reciprocating internal combustion engines but later the advances in turboshaft engines allowed it to be a far better choice. Light and robust rotor mechanism along with good aerodynamic efficiency was also a challenge. Another major problem was controlling helicopter during flight which could be summarized in both directional and altitude control[1, 2].

paragraph Complexity of rotor kinematics and aerodynamics caused more restrictive problems in developing helicopters such as lift asymmetry in forward flight, compared to a hovering flight as shown in Figure 1, resulting in rolling moment on helicopter disc rotor. Lift asymmetry was overcame by making the blade free to flap. Such solution was introduced using the flapping hinge which was first proposed by Cierva in 1922. Flapping hinge causes the relative angle of attack at retreating side of disc rotor to be decreased due to the upward motion of the blade (downward relative wind) and that at the advancing side to be increased in the same manner as shown of Figure 2. In forward flight, forward speed causes relative airspeed differences in tangential velocity at both sides on disc rotor[3, 4, 5].


Content from this work may be used under the terms of the Creative Commons Attribution 3.0 licence. Any further distribution of this work must maintain attribution to the author(s) and the title of the work, journal citation and DOI.
Published under licence by IOP Publishing Ltd

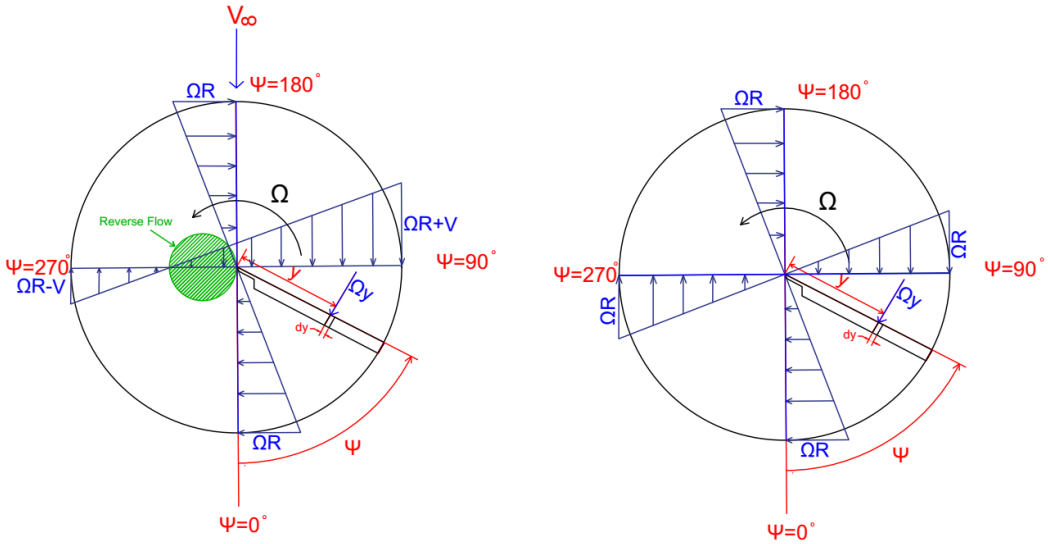

(a) Forward Flight (b) Hovering Flight

Figure 1. Helicopter Disc Rotor Velocity Distribution

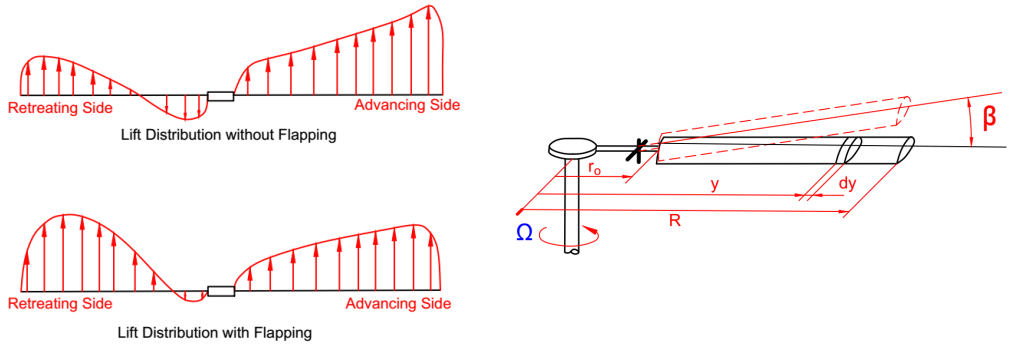

(a) Effect of Blade Flapping on Lateral Lift Distribution (b) Blade Flapping about Flapping Hinge

Figure 2. Blade Flapping in Forward Flight

In the past, experimental investigations on multiple helicopter models was the main tool for studying complex flowfield around rotorcrafts and prediction of rotor dynamics [6, 7, 8] but was a very expensive tool. In the 70s, ONERA applied of CFD to helicopter problems by considering Euler and Navier-Stokes equations that Renaud et al [9] used to solve the full flow field around a helicopter. A considered work using the coupling of computational fluid dynamics CFD with comprehensive analysis showed better predictions of aerodynamic loads on the UH-60A rotor [10], but it was time expensive. Semi-empirical models using unsteady aerodynamics considering dynamic stall [11, 12] were developed but failed to speculate stalled regimes if compared to experimental studies for the UH-60A [13].

Recently, numerical techniques, such as the Chimera[14], allowed for more reasonable modeling of the helicopter rotor. Also, experiments on biological flight for both insects and birds gained some interesting phenomena that also were modeled to be included in the design process. Flapping aerodynamics in forward flight were modeled and have been very well used in preliminary design procedures for ornithopters [15, 16, 17, 18].

Almost all analyses of helicopter aerodynamics started with blade element theory as it relates rotor performance and aerodynamic characteristics to the detailed design parameters. Blade element theory is basically lifting line theory applied to the rotating wings. It assumes that each blade strip is a two dimensional

airfoil that produces aerodynamic forces. The effect of rotor wake is accounted for in the relative angle of attack at each section in the form of induced angle of attack. Drzewiecki[19] was apparently the first one to consider the blade element theory for studying airplane propellers along with the contributions made by Lanchester[20]. Blade element theory (BET) gives an estimation of both radial and azimuthal loadings on rotor blade along the disc.

In the present paper, blade element theory is applied for helicopter rotor blade in forward flight. Relative angle of attack is calculated at each element and used for obtaining the elementary aerodynamic forces. As a first attempt, blade element theory is applied to 7A rotor high speed test (test point 312) and the results are compared to the experimental ones that was performed in ONERA S1MA transonic wind tunnel in 1991. The present effort insures the importance of blade element theory for preliminary design calculations of helicopter rotor blade.

2. Blade element theory

Each blade element section experiences a periodic change in its local velocity along with more affecting inputs such as blade flapping, compressibility effects, unsteady influence, stall regimes, reverse flow and induced velocities.

Rotor blade performance cannot be fully achieved that would match the reality so, multiple assumptions are considered in the present work that are:

- Rigid blade is considered in flapping motion (i.e. blade elasticity is neglected).
- Blade weight is ignored.
- Lead and lag rotor blade motions are neglected, (they are important in vibration and aeroelasticity problems.)
- Flapping hinge offset is ignored.
- Dynamic stall and compressibility are not accounted for in the present calculations.

As shown in figure 3, both velocities due to blade rotor rotation and the forward velocity of the helicopter itself form the tangential velocity, u_t. The tangential, perpendicular and radial velocity components on each element are given as function of azimuthal and radial positions as follows:

$$u_t(\psi, r) = \Omega y + u_\infty \, sin\, \psi \tag{1}$$

$$u_p(\psi, r) = (u_\infty \, \alpha_s - u_i) - r\, \dot{\beta} - u_\infty \, \beta \, cos\psi \tag{2}$$

$$u_R(\psi, r) = u_\infty \, cos\psi + (u_\infty \, \alpha_s - u_i)\beta \tag{3}$$

where Ω is the rotor angular velocity, y is the radial position, $r = \frac{y}{R}$ is the non-dimensional radial position, u_∞ is flight velocity, α_s is shaft angle of attack, u_i is the induced velocity, β and $\dot{\beta}$ are the flapping angle and flapping velocity respectively which are also function of both azimuthal position (ψ) and non-dimensional radial position (r). The flapping angle as was illustrated in Figure 2(b) is formulated in Fourier series[3] as follows:

$$\beta(\psi) = \beta_0 + \beta_{1c}\, cos\, \psi + \beta_{1s}\, sin\, \psi + \beta_{2c}\, cos\, 2\psi + \beta_{2s}\, sin\, 2\psi + ... \\ = \beta_0 + \sum_{n=1}^{\infty} (\beta_{nc}\ cos\, n\psi + \beta_{ns}\ sin\, n\psi) \tag{4}$$

where β_0 is the coning angle, β_{nc} is the longitudinal flapping and β_{ns} is the lateral flapping all are calculated as follows:

$$\beta_0 = \frac{1}{2\pi} \int_0^{2\pi} (\beta) d\psi \tag{5a}$$

$$\beta_{nc} = \frac{1}{\pi} \int_0^{2\pi} \beta\, cos\, (n\psi)\, d\psi \tag{5b}$$

$$\beta_{ns} = \frac{1}{\pi}\int_0^{2\pi} \beta \, sin\,(n\psi)\, d\psi \tag{5c}$$

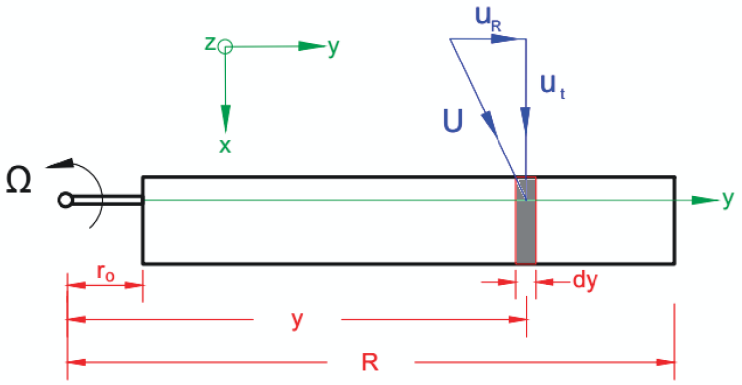

Figure 3. Rotor blade schematic drawing for BET

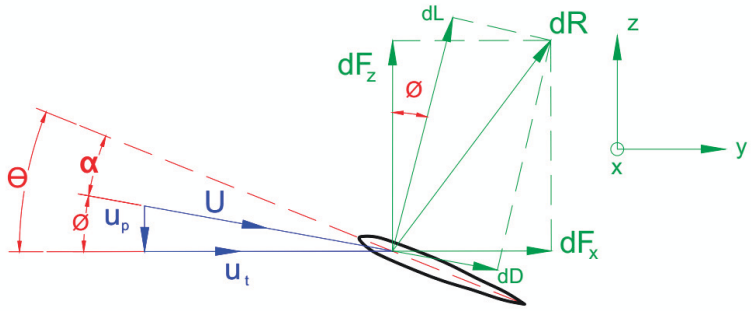

Figure 4. Aerodynamic forces and angles defined on blade element

Pitching motion is considered to be both collective or/and cyclic that is also presented in Fourier series form with the first harmonics only as follows:

$$\theta(\psi, r) = \theta_{tw}\, r + \theta_0 + \theta_{1c}\, cos\, \psi + \theta_{1s}\, sin\, \psi \tag{6}$$

where θ_{tw} is the linear twist, θ_0 is the collective pitch, θ_{1c} is lateral cyclic and θ_{1s} is the longitudinal cyclic.

Thus the relative angle of attack can be written as:

$$\alpha(\psi, r) = \theta(\psi, r) + tan^{-1}(\frac{u_p(\psi, r)}{u_t(\psi, r)}) = \theta(\psi, r) + \phi(\psi, r) \tag{7}$$

By substituting for u_p, the relative angle of attack will be:

$$\alpha = \theta(\psi, r) - tan^{-1}(\frac{(u_\infty\, \alpha_s - u_i) - r\, \dot{\beta} - u_\infty\, \beta\, cos\psi}{u_t}) \tag{8}$$

Considering airfoil characteristics of each element, the resultant elementary lift dL and drag dD per unit span on this blade element will be

$$dL = \frac{1}{2}\rho\, U^2\, c\, C_l\, dy \tag{9}$$

$$dD = \frac{1}{2}\rho\, U^2\, c\, C_d\, dy \tag{10}$$

where U is the resultant velocity and equals $\sqrt{u_t^2 + u_p^2}$, C_l and C_d are lift and drag coefficients simultaneously and both are obtained for each section of the rotor blade according to sectional airfoil characteristics.

By resolving the two forces, lift and drag, into parallel and normal to the rotor disk:

$$dF_z = dL\, cos\phi - dD\, sin\phi \tag{11}$$

$$dF_x = dL\, sin\phi + dD\, cos\phi \tag{12}$$

Therefore, the elementary thrust, torque, and power of the disk are:

$$dT = (dL\, cos\phi - dD\, sin\phi) \tag{13}$$

$$dQ = (dL\, sin\phi + dD\, cos\phi)y \tag{14}$$

$$dP = (dL\, sin\phi + dD\, cos\phi)\Omega\, y \tag{15}$$

The instantaneous thrust, torque, and power of the disk are obtained by integrating radially as shown:

$$T(\psi) = \int_{r_0}^{R} dT \tag{16}$$

$$Q(\psi) = \int_{r_0}^{R} dQ \tag{17}$$

$$P(\psi) = \int_{r_0}^{R} dP \tag{18}$$

Finally, the rotor's average thrust, torque and power can be obtained by integrating T(t), Q(t) and P(t) over the whole cycle for all the blades.

$$\overline{T} = \frac{N_b}{2\pi}\int_0^{2\pi} T(\psi)d\psi \tag{19}$$

$$\overline{Q} = \frac{N_b}{2\pi}\int_0^{2\pi} Q(\psi)d\psi \tag{20}$$

$$\overline{P} = \frac{N_b}{2\pi}\int_0^{2\pi} P(\psi)d\psi \tag{21}$$

where N_b is the number of the blades.

3. 7A rotor high speed test

The wind-tunnel test of ONERA 7A rotor are used to determine the accuracy of blade element theory for calculating the local aerodynamic forces. The tests were implemented in 1991 in ONERA S1MA[21] that is a transonic closed-circuit wind tunnel with a circular cross section of $8\ \ m$ diameter. 7A rotor geometric characteristics are presented in Table 1 and shown in Figure 5, high speed test point 312 operational conditions are shown in Table 2. The 7A rotor has OA213 airfoil from blade root to 75% of rotor radius and OA209 airfoil from 90% of rotor radius to blade tip with a linearly interpolated profile between the two profiles. The measurements were conducted using pressure transducers at five blade sections (r/R = 0.975, 0.915, 0.825, 0.700 and 0.500)[22].

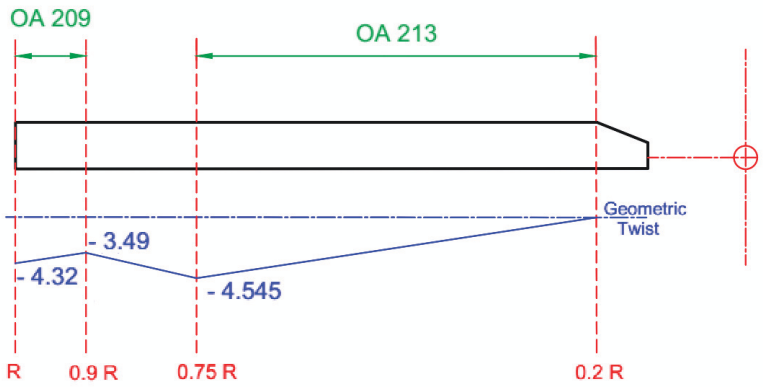

Figure 5. Geometric Characteristics of 7A Rotor blade

Table 1. 7A Rotor Geometric Characteristics

Parameter	Value	Definition
R	$2.1\ m$	Radius of Rotor
σ	0.084	Rotor solidity
c	$0.14\ mm$	Blade Chord
N_b	4	Rotor Number of blades

Table 2. ONERA 7A High Speed Test point 312 Operational Conditions

Parameter	Value	Definition
θ_0	$10.41°$	Collective pitch angle
θ_{1c}	$3.43°$	Lateral cyclic
θ_{1s}	$-3.7°$	Longitudinal cyclic
α_s	$-13.75°$	Shaft angle of attack
β_{1c}	$= \theta_{1s} = -3.7°$	Longitudinal Flapping
β_{1s}	0	Lateral Flapping
Ω	$106\ rad/s$	Rotational speed
μ	0.4	Tip speed ratio

Both longitudinal and lateral flapping coefficients (β_{1c}, β_{1s}) were trimmed to be $\beta_{1c} = \theta_{1s},\ \beta_{1s} = 0$ as shown in the Table 2, which is called the Modane Flapping Law[21]. The coning angle is assumed to be $8.9°$. The pitching and flapping motions are given by:

$$\theta(\psi) = 10.41° + 3.43°\ cos(\psi) - 3.7°\ sin(\psi) \tag{22}$$

$$\beta(\psi) = 8.9° - 3.7°\ cos(\psi) \tag{23}$$

The induced velocity variation radially and azimuthally is is assumed to be:

$$u_i = \frac{C_T}{\mu}(1 + r\ cos\psi) \tag{24}$$

4. Results and Discussion

Blade element theory is applied in the the present effort for calculating multiple variables along both the azimuth and the radial positions. Relative angle of attack depends mainly on three variable parameters that are the pitch angle, θ, tangential velocity, u_t, and perpendicular velocity, u_p as was presented in Eqn.7. The mentioned three parameters are illustrated in Figure 6 as function of both the azimuth and radial positions.

Figure 6(a) shows the pitch angle which changes radially according to the geometric twist and azimuthally due to longitudinal and lateral cyclic. The pitch angle decreases, along the azimuth, in the advancing side and increases in the retreating one. In Figure 6(b) and Figure 6(c) the tangential and perpendicular velocities are illustrated respectively as well as the pitch angle.

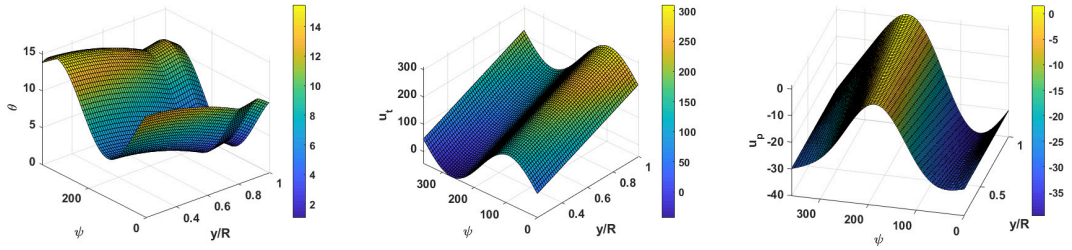

(a) Pitch Angle (b) Tangential Velocity (c) Perpendicualr Velocity

Figure 6. Discwise and Radial Variations of Motion Kinematics

The relative angle of attack variation along both the radius and the azimuth is presented in Figure 7(a) which shows the stall regions near the blade root in the retreating phase due to high angles of attack at reverse flow region. Positive and negative high angles of attack are shown in the stall region due to the small positive and negative values of the tangential velocities in small vicinities of the zero velocity boundary of the reversed flow region. As desired, the relative angle of attack decreases on the advancing side of the disc and increases on the retreating side as figured in Figure 8(a) in which the relative angle of attack is plotted for five different radii.

Local normal force variation is needed in designing helicopter rotors which is needed to be nondimensionalized so non dimensional normal force, $C_n.M^2$, is proposed as follows:

$$C_n.M^2 = \frac{N}{\frac{1}{2}\rho\, a_\infty^2\, c\, dy} \tag{25}$$

where, M is Mach number, N is the local normal force (normal to the chord), a_∞ is the local speed of sound and dy is the elementary radius (width of each element). Figure 7(b) shows the variation of non-dimensional normal force both azimuthally and radially then also as for relative angle of attack, it's plotted for five different radii in Figure 8(b) with which test point 312 will be compared in Figure 9.

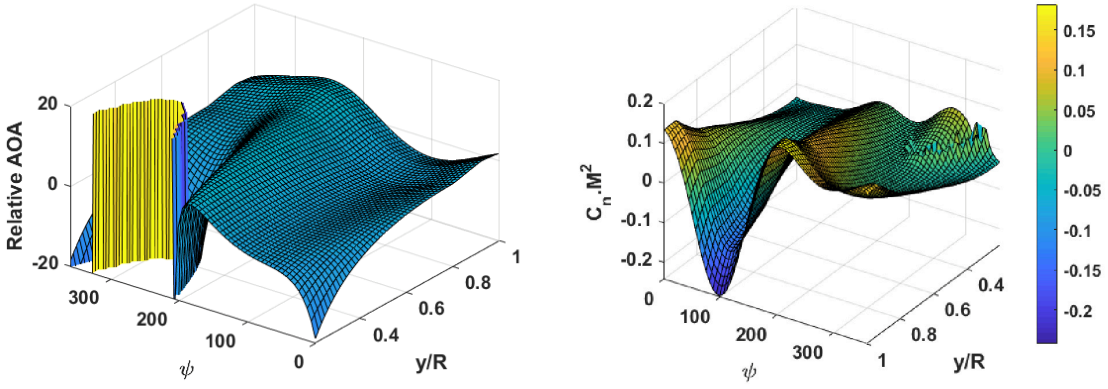

(a) Relative AOA (b) Non-dimensional Normal Lift Coefficient

Figure 7. Discwise and Radial Variations of Relative Angle of Attack and Non-dimensional normal force coefficient

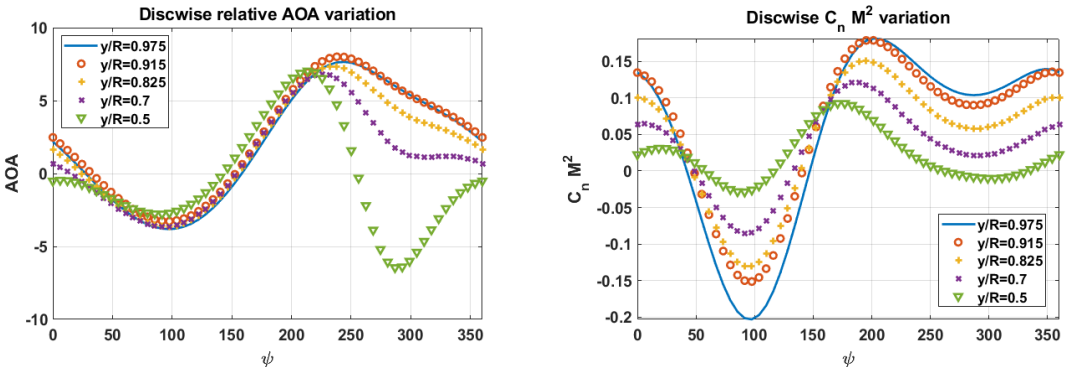

(a) Relative AOA (b) Non-dimensional Normal Lift Coefficient

Figure 8. Discwise Variations of Relative Angle of Attack and Non-dimensional Normal Force Coefficient at Radii ($y/R = 0.975, y/R = 0.915, y/R = 0.825, y/R = 0.7, y/R = 0.5$)

Figure 9 shows the comparison between non-dimensional normal force from blade element theory and experimental results at nondimenstional radii of $y/R = 0.975, y/R = 0.915, y/R = 0.825, y/R = 0.7$ and $y/R = 0.5$). Blade element theory predicts the same pattern as the experimental but with a phase shift between the first peaks with also amplitude difference of non-dimensional normal force values than the experimental. The comparison insures blade element theory importance for preliminary design of helicopter rotors.

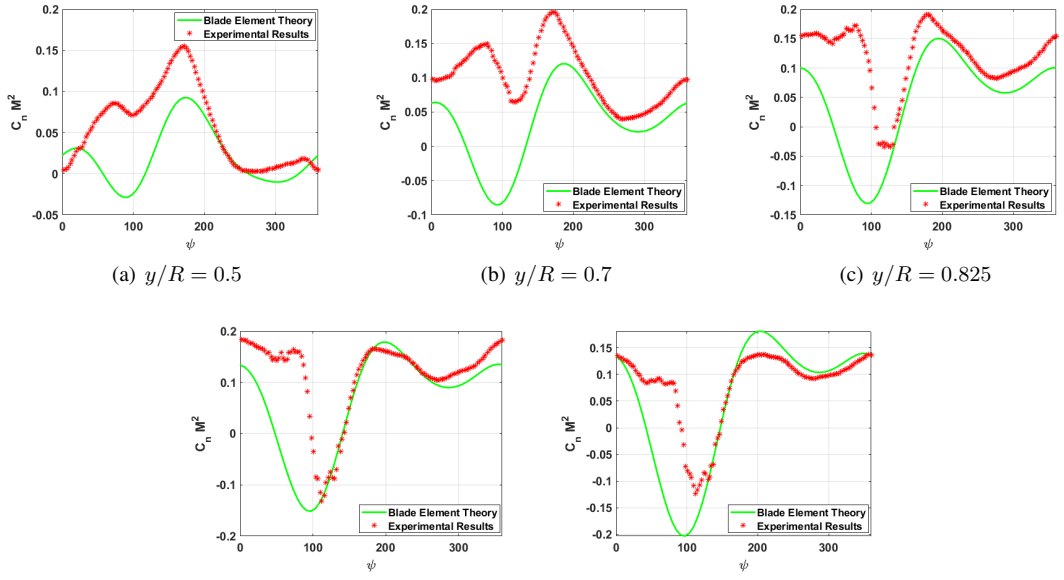

(a) $y/R = 0.5$ (b) $y/R = 0.7$ (c) $y/R = 0.825$

(d) $y/R = 0.915$ (e) $y/R = 0.975$

Figure 9. Comparisons of Blade Element Theory Results with 7A Rotor Test Data

5. Conclusion

Blade element theory is modeled for calculating the local non dimensional aerodynamic loads and also the average lift, thrust, power for rotary wings. The results were compared with 7A rotor experimental results at five non dimensional radial positions in high speed forward flight and showed the same pattern of variation along the azimuth which insures the importance of blade element theory for preliminary design. A convergence between blade element theory results and experimental ones is noted for higher radii due to the rigid blade consideration. Difference in values of both results in noted which can be referred to the considered assumptions in calculations even though the results give a good estimation of the local loads on helicopter rotor.

6. References

[1] Johnson, W., *Helicopter theory*, Courier Corporation, 2012.
[2] Padfield, G. D., *Helicopter flight dynamics: the theory and application of flying qualities and simulation modelling*, John Wiley & Sons, 2008.
[3] Leishman, G. J., *Principles of helicopter aerodynamics with CD extra*, Cambridge university press, 2006.
[4] Gessow, A. and Myers, G. C., *Aerodynamics of the Helicopter*, Frederick Ungar, 1952.
[5] Prouty, R. W., *Helicopter performance, stability, and control*, 1995.
[6] Sheridan, P. F. and Smith, R. P., "Interactional aerodynamicsa new challenge to helicopter technology," *Journal of the American Helicopter Society*, Vol. 25, No. 1, 1980, pp. 3–21.
[7] Berry, J. D. and Althoff, S. L., "Inflow velocity perturbations due to fuselage effects in the presence of a fully interactive wake," 1990.
[8] Berry, J. D. and Bettschart, N., "Rotor-fuselage interaction: Analysis and validation with experiment," 1997.
[9] Renaud, T., Benoit, C., Boniface, J.-F., and Gardarein, P., "Navier-Stokes computations of a complete helicopter configuration accounting for main and tail rotors effects," 2003.
[10] Potsdam, M., Yeo, H., and Johnson, W., "Rotor airloads prediction using loose aerodynamic/structural coupling," *Journal of Aircraft*, Vol. 43, No. 3, 2006, pp. 732–742.
[11] Petot, D., "Modélisation du décrochage dynamique par équations différentielles," *La Recherche Aérospatiale*, , No. 5, 1989, pp. 59–72.
[12] Truong, V., "A 2-d dynamic stall model based on a hopf bifurcation," *European Rotorcraft Forum*, Vol. 19, ASSOCIAZIONE ITALIANA DI AERONAUTICA ED ASTRONAUTICA, 1993, pp. C23–C23.
[13] Nguyen, K. and Johnson, W., "Evaluation of dynamic stall models with UH-60A airloads flight test data," *Annual forum proceedings-American helicopter society*, Vol. 54, AMERICAN HELICOPTER SOCIETY, 1998, pp. 576–588.
[14] Boniface, J.-C., Guillen, P., Le Pape, M., Darracq, D., and Beaumier, P., "Development of a chimera unsteady method for the numerical simulation of rotorcraft flowfields," *36th AIAA Aerospace Sciences Meeting and Exhibit*, 1998, p. 421.
[15] Zakaria M.Y., Elshabka A.M., B. A. and O.E., A. E., "Numerical Aerodynamic Characteristics of Flapping Wings," *13th International Conference on Aerospace Sciences & Aviation Technology, ASAT-13, May*, Vol. 26, 2009, p. 15.
[16] Stewart, E. C., Patil, M. J., Canfield, R. A., and Snyder, R. D., "Aeroelastic Shape Optimization of a Flapping Wing," 2014.
[17] Zakaria M.Y., Bayoumy A.M., E. A. and O.E, A. E., "Experimental Aerodynamic Characteristics of Flapping Membrane Wings," *13th International Conference on Aerospace Sciences & Aviation Technology, ASAT-13, May*, Vol. 26, 2009, p. 18.
[18] Zakaria, M. Y., Taha, H. E., and Hajj, M. R., "Design Optimization of Flapping Ornithopters: The Pterosaur Replica in Forward Flight," *Journal of Aircraft*, Vol. 53, No. 1, 2016, pp. 48–59.
[19] Drzewiecki, S., "Théorie générale de l'hélice: Hélices aériennes et hélices marines. Par S. Drzewiecki," 1920.
[20] Lanchester, F. W., "A contribution to the theory of propulsion and the screw propeller," *Journal of the American Society for Naval Engineers*, Vol. 27, No. 2, 1915, pp. 509–510.
[21] Costes, J.-J., "AERODYNAMIC MOMENTS ON ROTOR BLADES IN FORWARD FLIGHT: TEST RESULTS AND MODELING," , No. 11, 1995.
[22] Tourjansky, N. and Szechenyi, E., "The measurement of blade deflections-a new implementation of the strain pattern analysis," *ONERA TP*, 1992.